

Figure 1: Simulated surface concentrations ($\times 10^6$ molec cm^{-3}) of OH for January and July months.

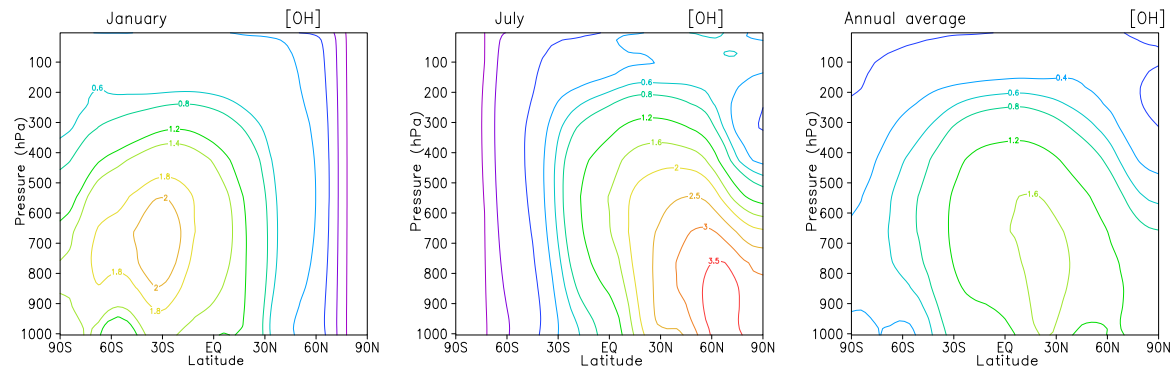


Figure 2: Simulated zonal mean concentration of OH ($\times 10^6$ molec cm^{-3}) for January, July, and annual average.

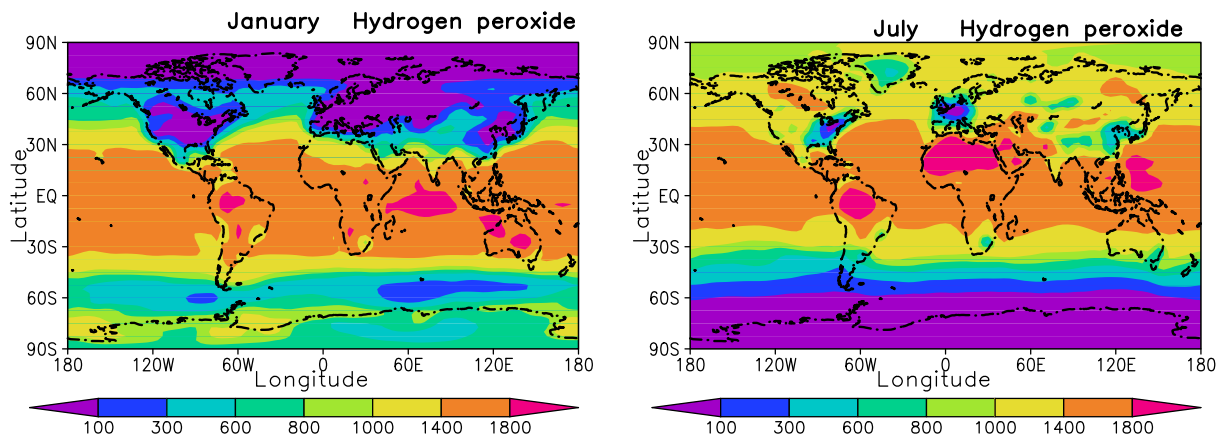


Figure 3: Simulated surface concentration (pptv) of H_2O_2 for January and July.

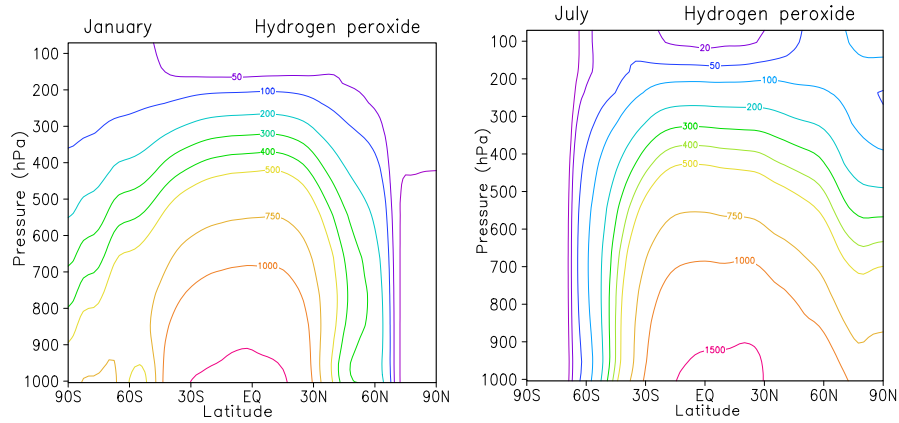


Figure 4: Simulated zonal mean concentration of H_2O_2 (pptv) for January and July.

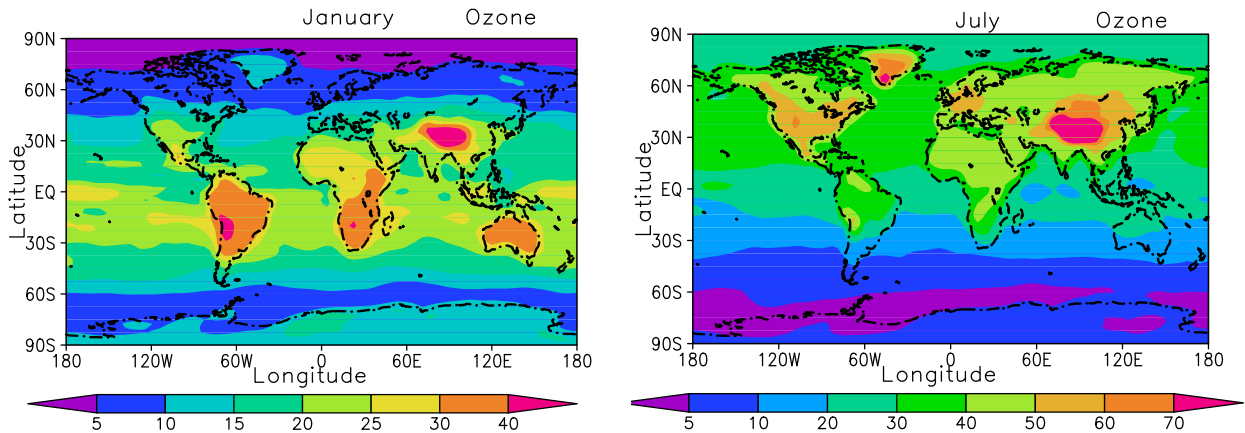


Figure 5: Simulated surface concentration (ppbv) of O_3 for January and July.

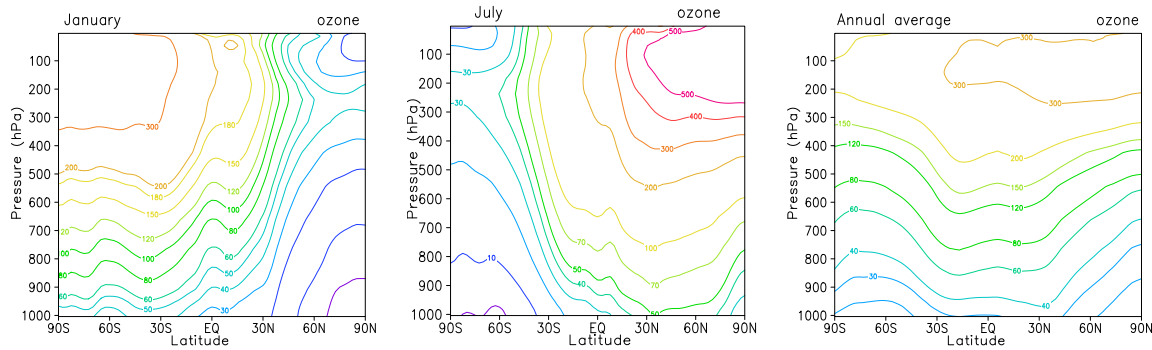


Figure 6: Simulated zonal mean concentration of O_3 (ppbv) for January, July, and annual average.

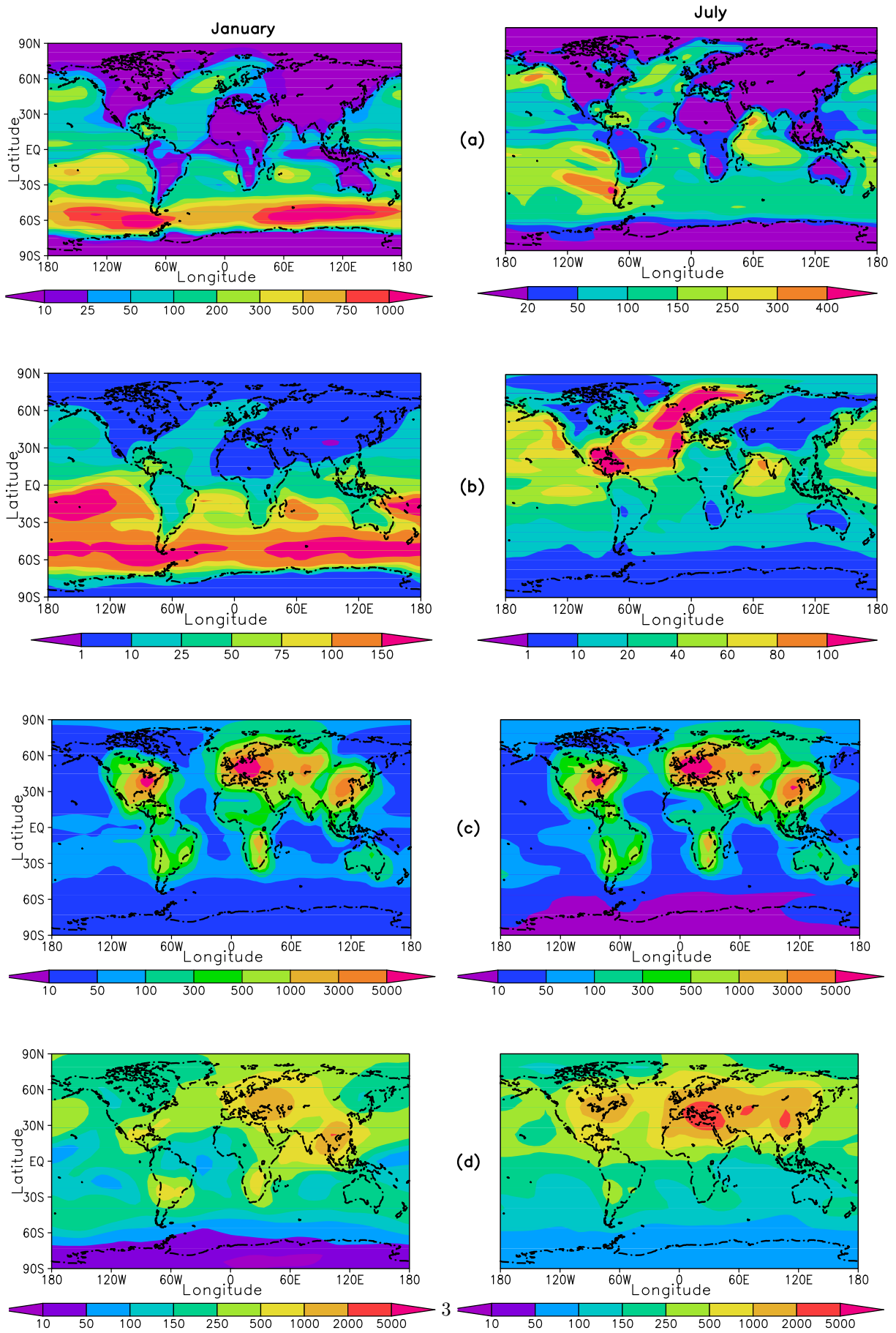


Figure 7: Simulated mean concentration (pptv) of (a) DMS, (b) MSA, (c) SO₂, and (d) sulfate for January and July.

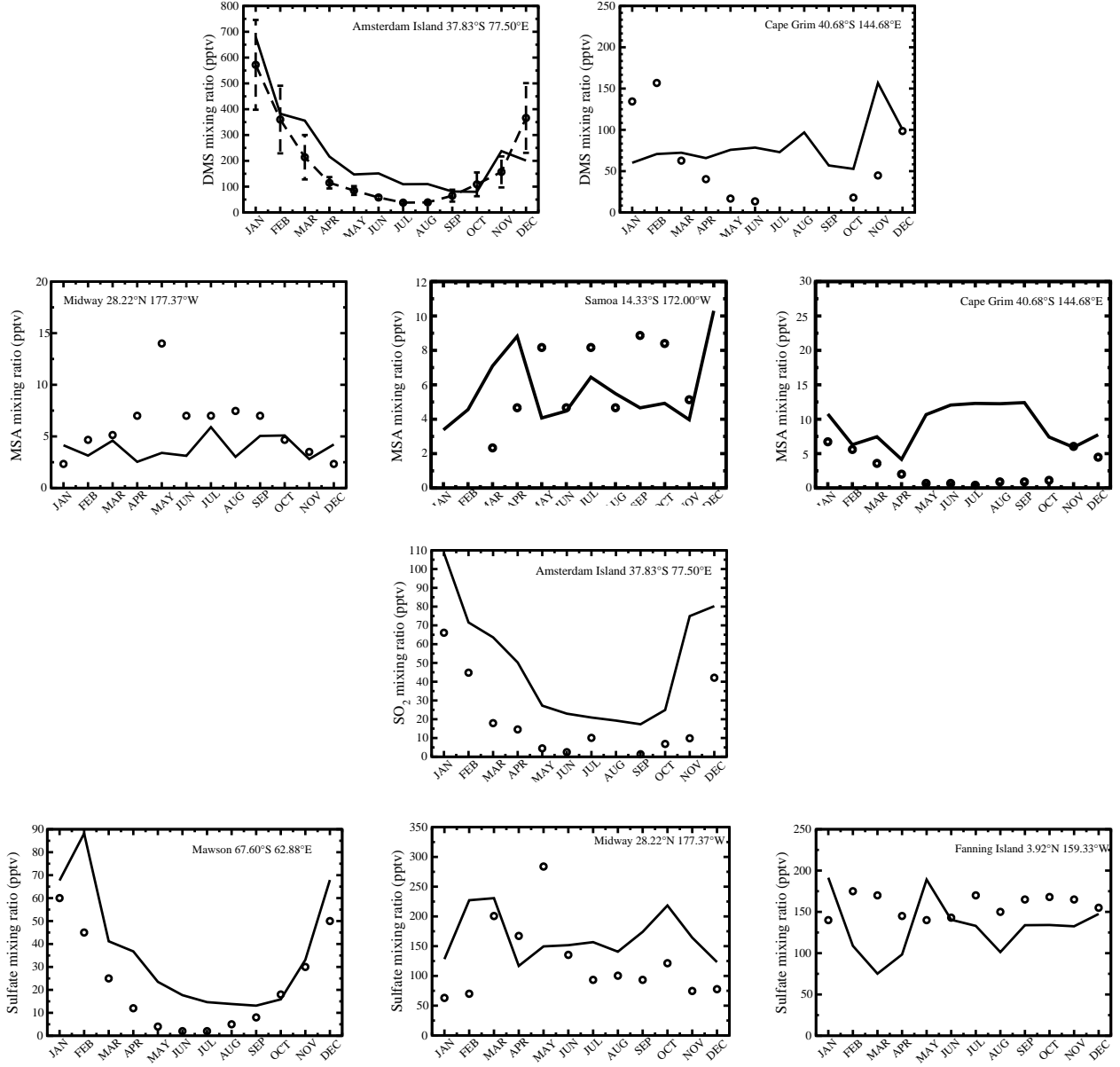


Figure 8: Comparison of seasonal DMS, MSA, SO₂, and sulfate mixing ratios (pptv) with measurements. The open circles and solid lines indicate monthly mean observed and modeled mixing ratios, respectively.

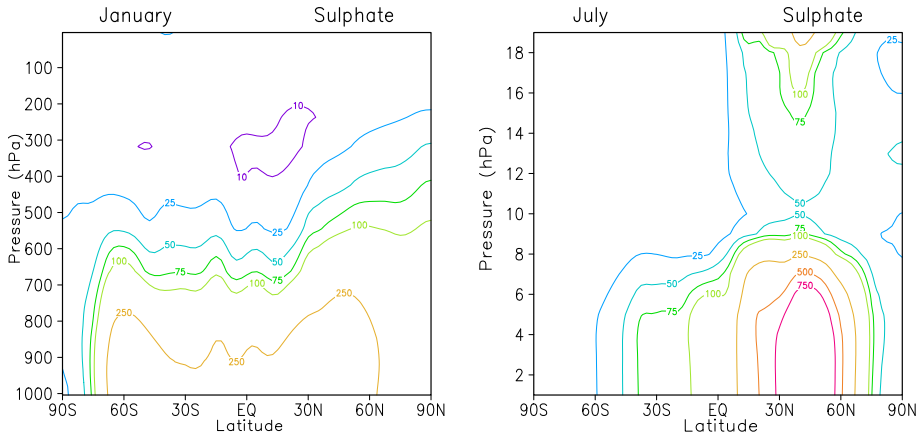


Figure 9: Simulated zonal mean concentration of sulfate (pptv) for January and July.

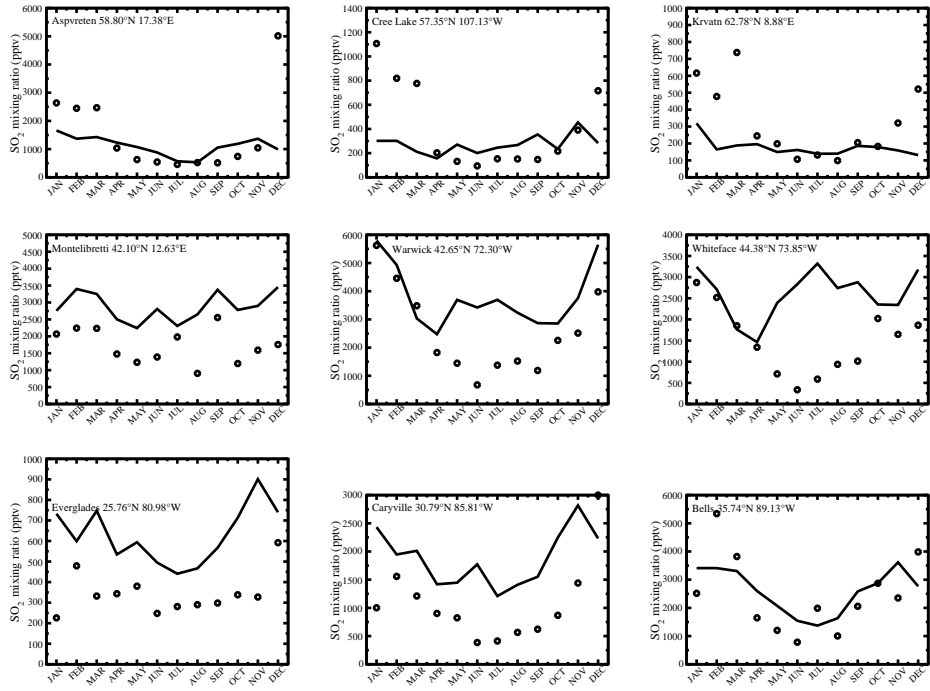


Figure 10: Modeled (open circles) and observed (solid line) concentrations (pptv) of SO_2 circles: upper panel: Aspvreten, Cree Lake, Kravatn; middle panel: Montelibretti, Warwick, Whiteface; lower panel: Everglades, Caryville, Bells (from left to right).

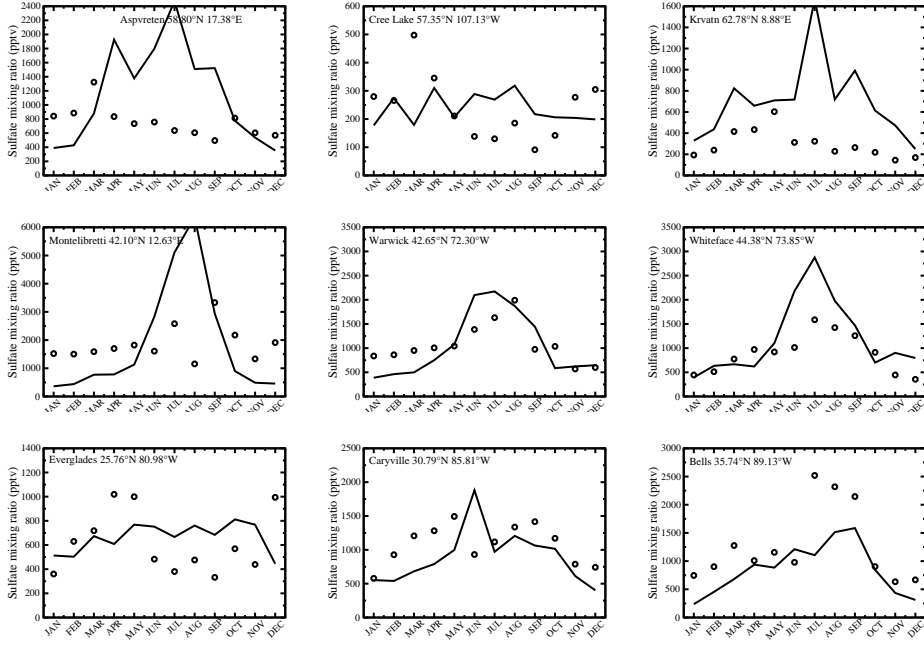


Figure 11: Same as Fig. 11 but for sulfate (pptv).

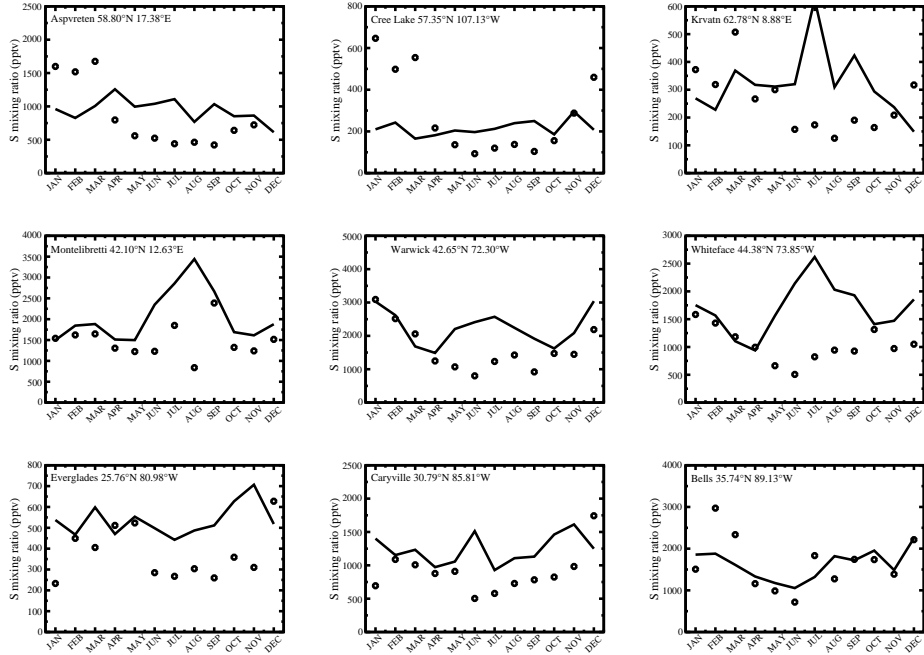


Figure 12: Total sulfur, sum SO₂ and sulfate given in Figs. 10 and 11, respectively.

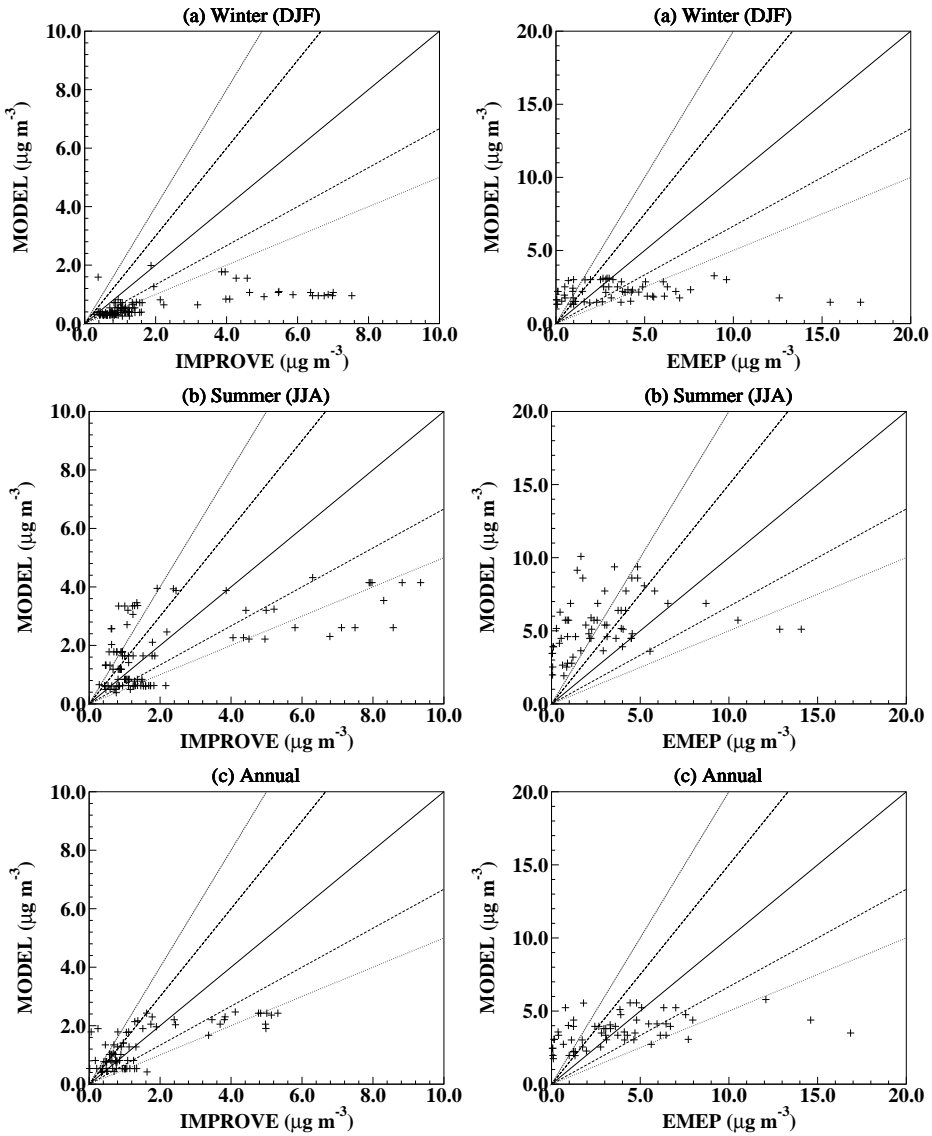


Figure 13: Scatter of observed vs modeled sulfate concentrations over North America and Europe.

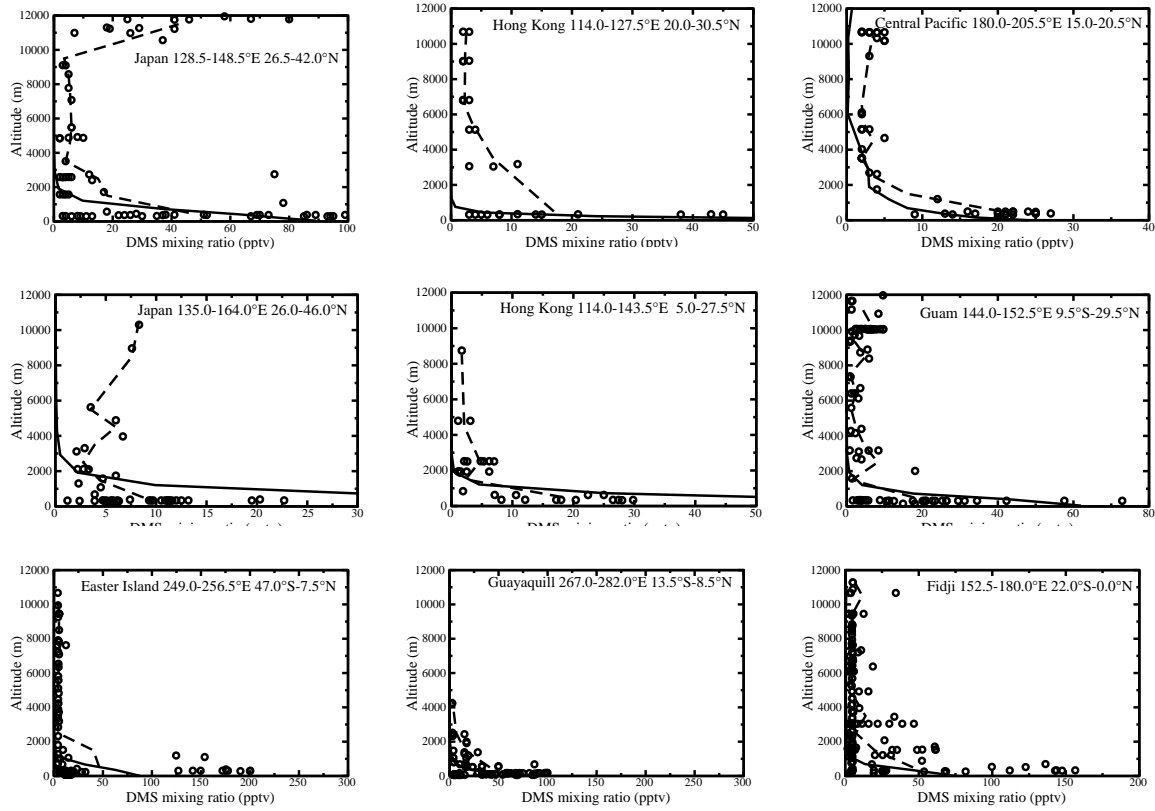


Figure 14: Comparison of modeled DMS vertical profiles with measurements during the PEM-West A (upper panel), PEM-West B (upper panel), PEM-Tropics A (lower panel) field campaigns. Model results averaged over the region for the month of measurements are indicated by solid line. The observed mixing ratios averaged over altitudinal bands of 1 km are shown with a dashed line.

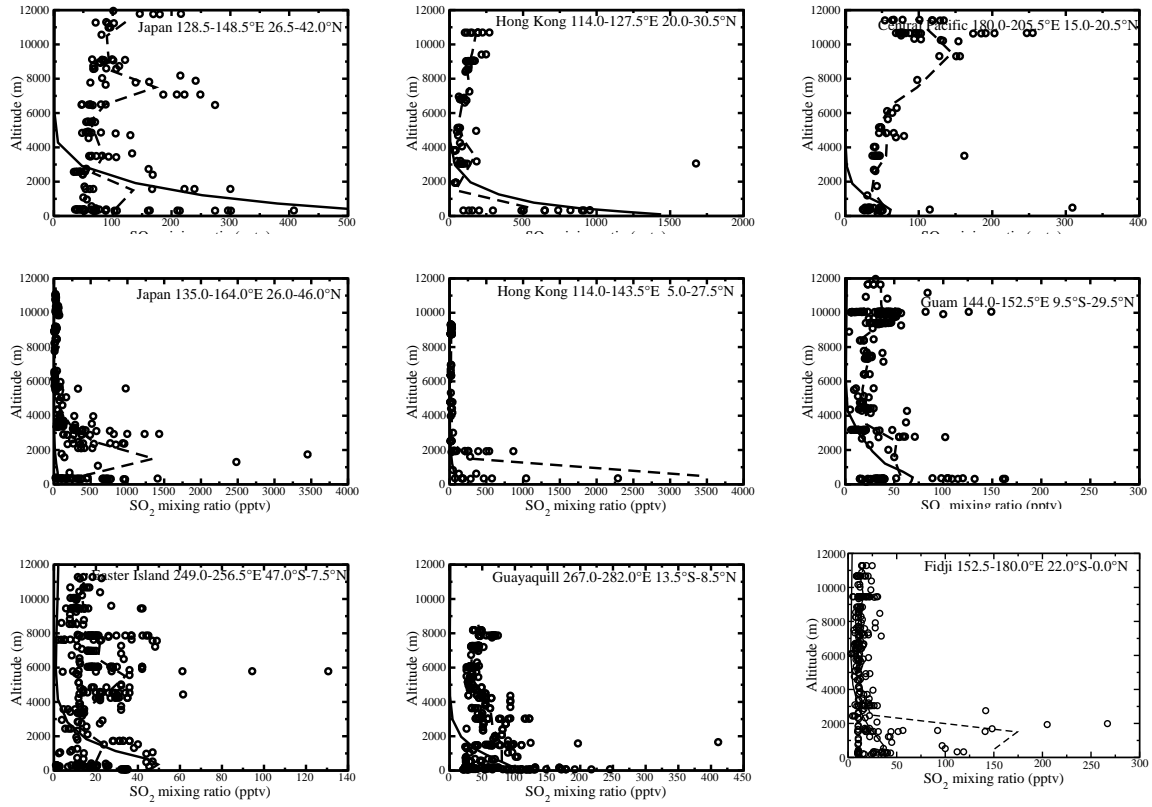


Figure 15: Same as Fig. 14 but for SO_2 .

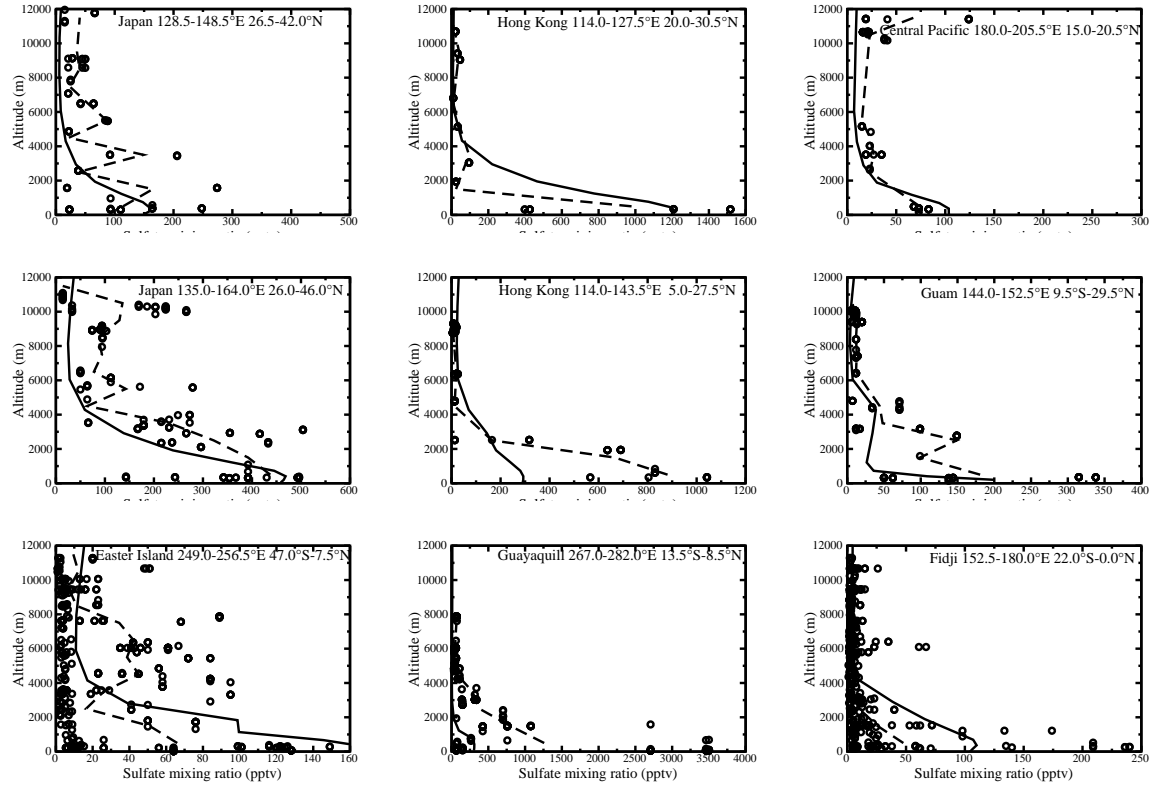


Figure 16: Same as Fig. 14 but for sulfate.

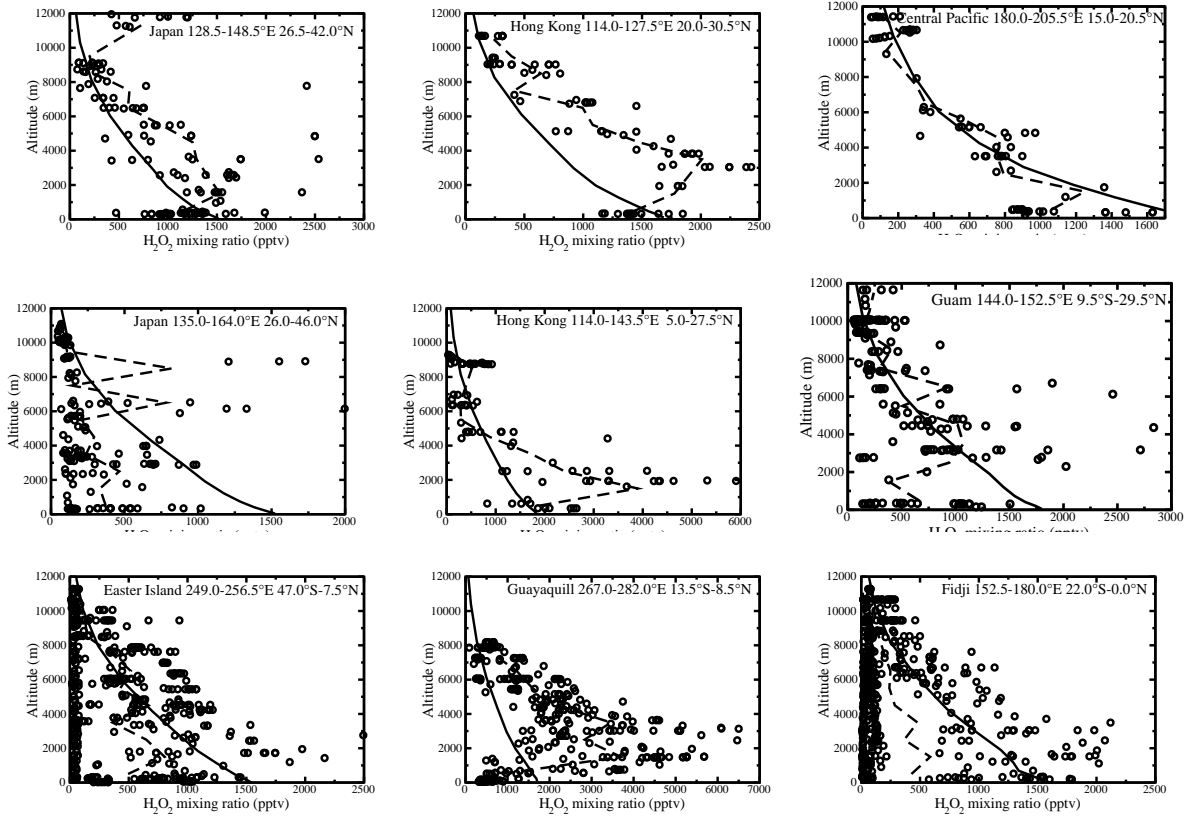


Figure 17: Same as Fig. 14 but for H_2O_2 .

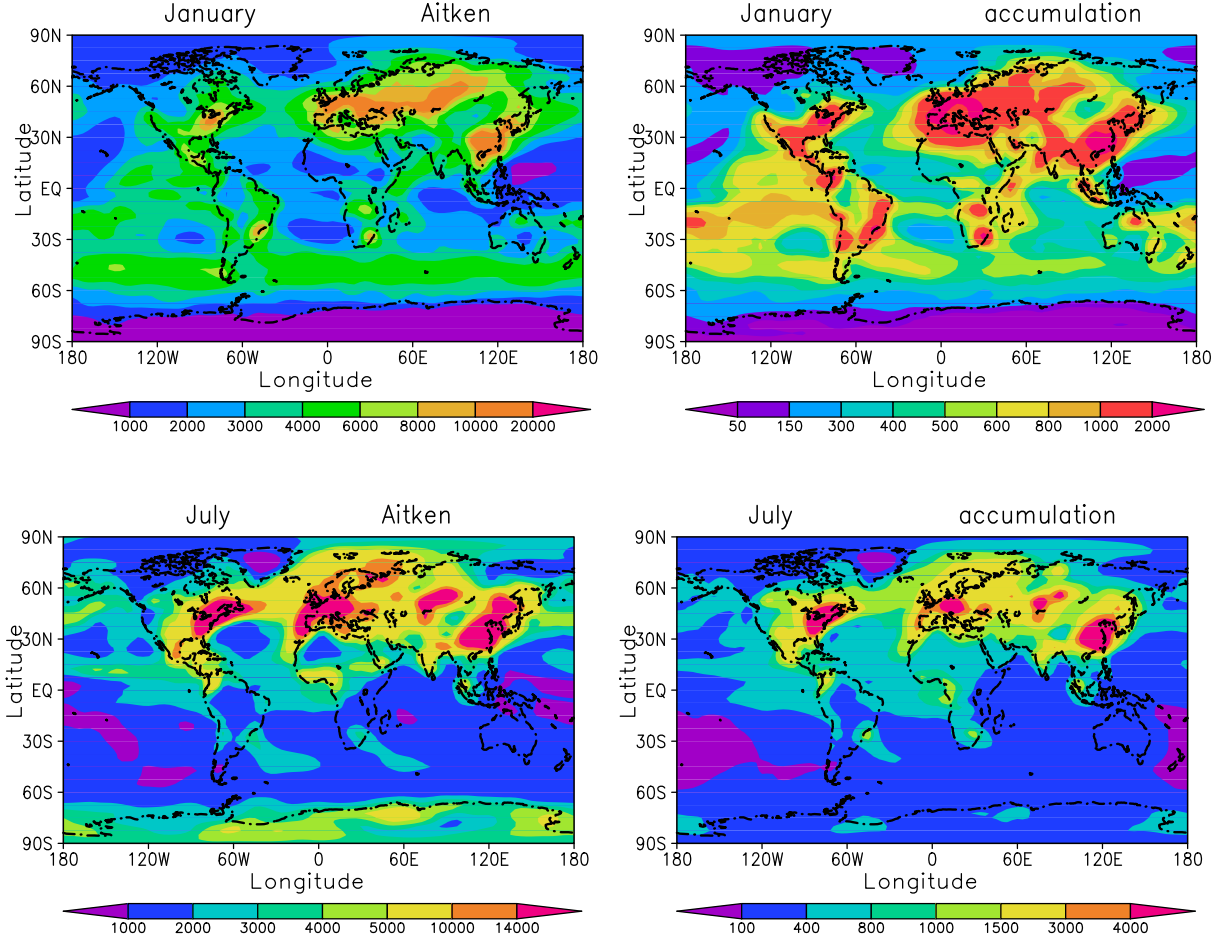


Figure 18: Modeled average sulfate number concentration (particles cm^{-3}) at surface for January and July months in Aitken and accumulation modes.

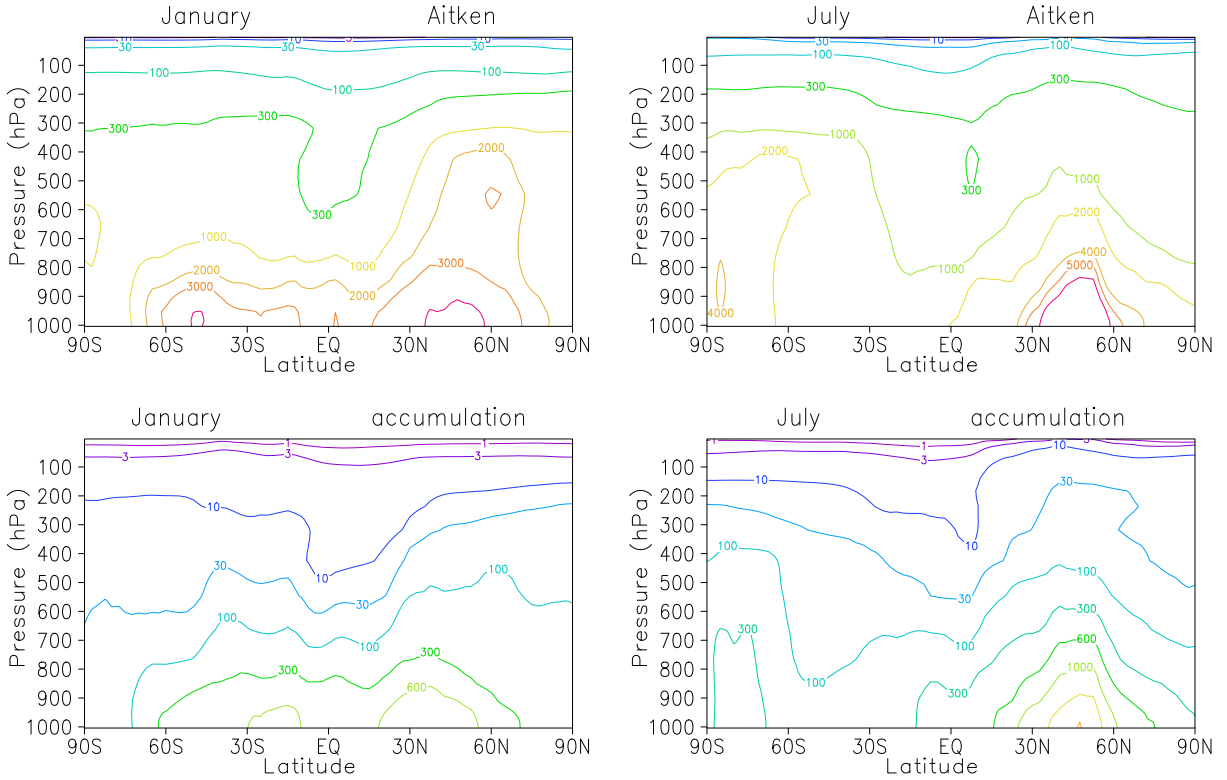


Figure 19: Zonally average simulated sulfate number concentration (particles cm^{-3}) for January and July months of Aitken and accumulation modes.

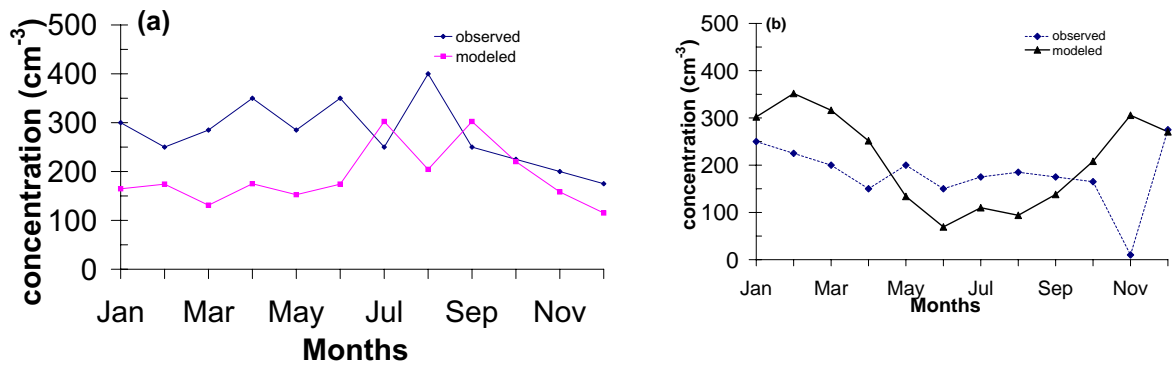


Figure 20: Number concentration (particles cm^{-3}) at (a) Mauna Loa and (b) American Samoa. Observations are from Wilson et al. [2001] for 1987.

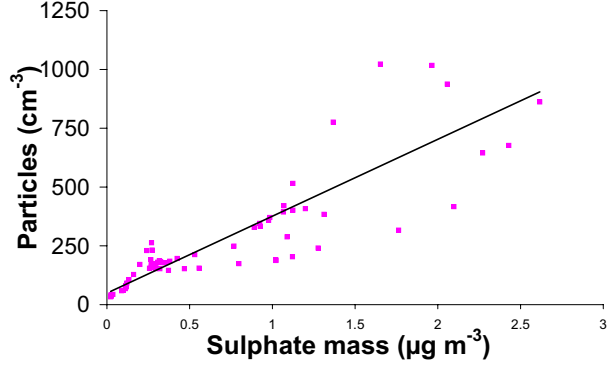


Figure 21: Simulated number concentration (particles cm^{-3}) to sulfate mass concentration ratios for the North Atlantic.

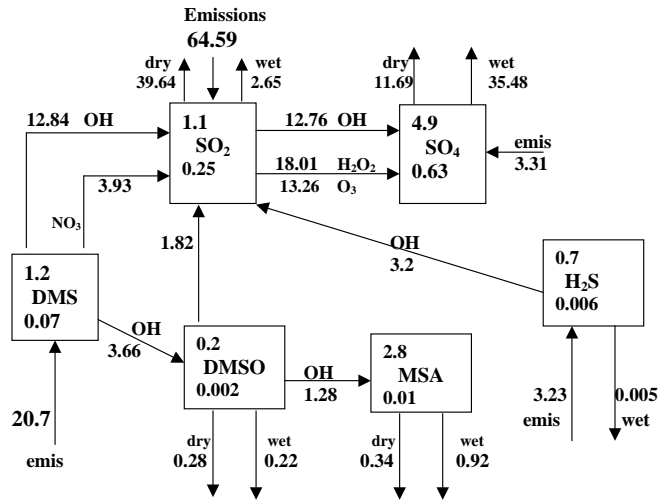


Figure 22: Globally and annually-averaged simulated sulphur budget. Burdens are given in TgS, fluxes in Tg S yr^{-1} , and lifetimes in days. Dry and Wet stands for dry and wet depositions, respectively.

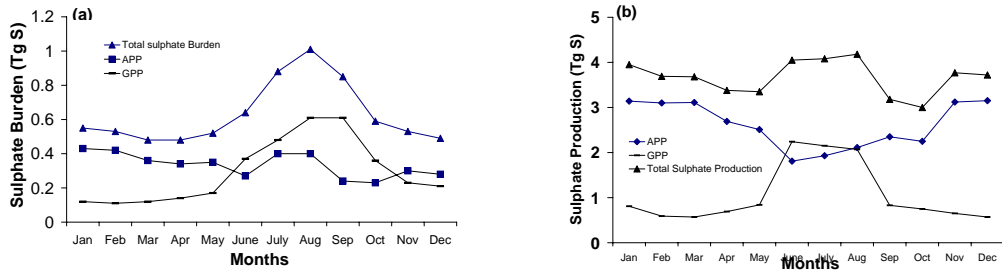


Figure 23: Monthly evolution of (a) sulfate burden and (b) production rate (TgS).

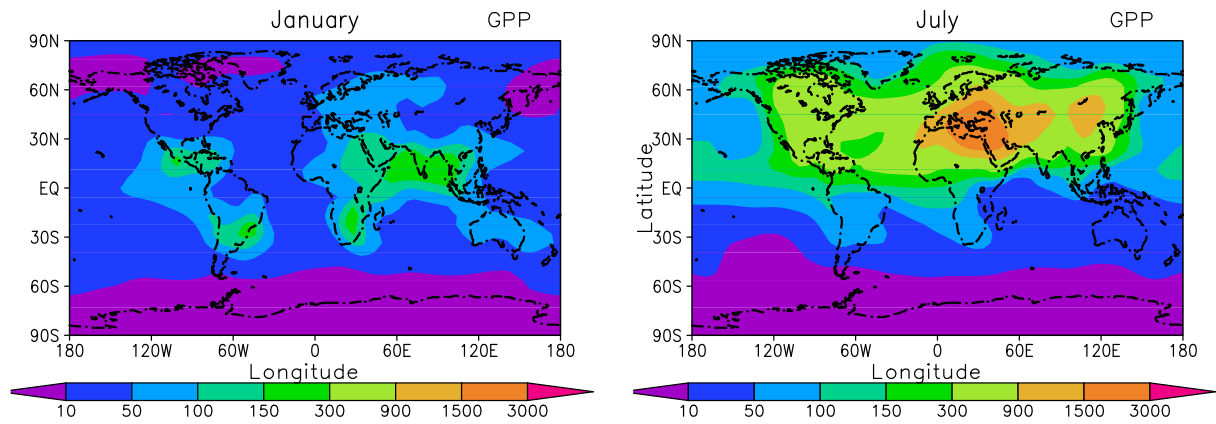


Figure 24: Simulated surface sulfate concentrations by gas-phase (pptv) for January and July months.

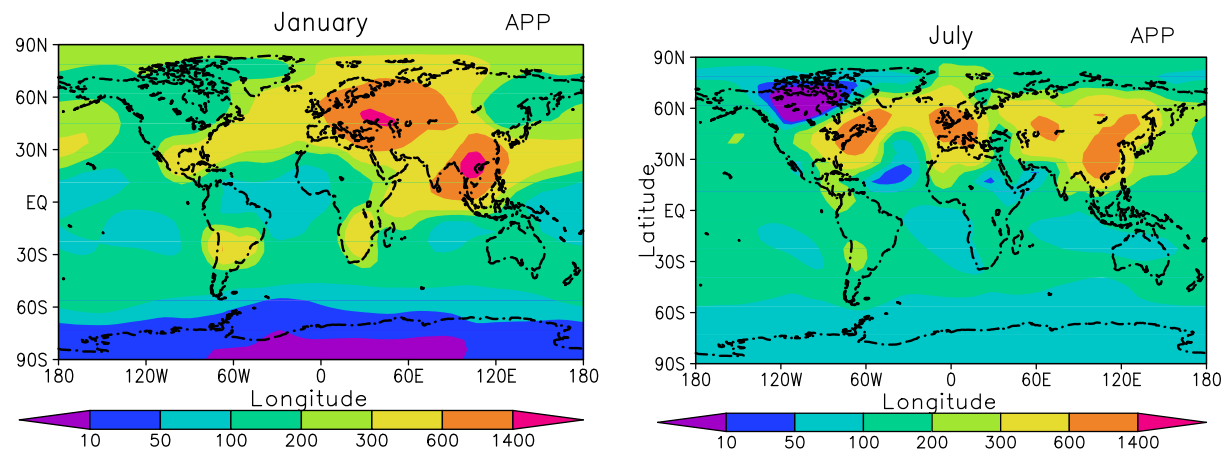


Figure 25: Simulated surface sulfate concentrations by aqueous-phase (pptv) for January and July months.